Distributed MAC Protocol for Cognitive Radio Networks: Design, Analysis, and Optimization

Le Thanh Tan, *Student Member, IEEE*, and Long Bao Le, *Member, IEEE*

***Abstract*—In this paper, we investigate the joint optimal sensing and distributed Medium Access Control (MAC) protocol design problem for cognitive radio (CR) networks. We consider both scenarios with single and multiple channels. For each scenario, we design a synchronized MAC protocol for dynamic spectrum sharing among multiple secondary users (SUs), which incorporates spectrum sensing for protecting active primary users (PUs). We perform saturation throughput analysis for the corresponding proposed MAC protocols that explicitly capture the spectrum-sensing performance. Then, we find their optimal configuration by formulating throughput maximization problems subject to detection probability constraints for PUs. In particular, the optimal solution of the optimization problem returns the required sensing time for PUs' protection and optimal contention window to maximize the total throughput of the secondary network. Finally, numerical results are presented to illustrate developed theoretical findings in this paper and significant performance gains of the optimal sensing and protocol configuration.**

***Index Terms*—Cognitive radio (CR), Medium Access Control (MAC) protocol, optimal sensing, spectrum sensing, throughput maximization.**

I. Introduction

EMERGING broadband wireless applications have demanded an unprecedented increase in radio spectrum resources. As a result, we have been facing a serious spectrum shortage problem. However, several recent measurements have revealed very low spectrum utilization in most useful frequency bands [1]. To resolve this spectrum shortage problem, the Federal Communications Commission (FCC) has opened licensed bands for unlicensed users' access. This important change in spectrum regulation has resulted in growing research interests on dynamic spectrum sharing and cognitive radio (CR) in both industry and academia. In particular, IEEE has established an IEEE 802.22 workgroup to build the standard for wireless regional area networks (WRANs) based on CR techniques [2].

Hierarchical spectrum sharing between primary and secondary networks is one of the most widely studied dynamic spectrum-sharing paradigms. For this spectrum-sharing paradigm, primary users (PUs) typically have strictly higher priority than secondary users (SUs) in accessing the underlying spectrum. One potential approach for dynamic spectrum sharing is to allow both primary and secondary networks to simultaneously transmit on the same frequency with appropriate interference control to protect the primary network [3], [4]. In particular, it is typically required that a certain interference temperature limit due to SUs' transmissions must be maintained at each primary receiver. Therefore, power allocation for SUs should carefully be performed to meet stringent interference requirements in this spectrum-sharing model.

Instead of imposing interference constraints for PUs, spectrum sensing can be adopted by SUs to search for and exploit spectrum holes (i.e., available frequency bands) [5], [6]. Several challenging technical issues are related to this spectrum discovery and exploitation problem. On one hand, SUs should spend sufficient time for spectrum sensing so that they do not interfere with active PUs. On the other hand, SUs should efficiently exploit spectrum holes to transmit their data by using an appropriate spectrum-sharing mechanism. Although these aspects are tightly coupled with each other, they have not thoroughly been treated in the existing literature.

In this paper, we make a further bold step in designing, analyzing, and optimizing Medium Access Control (MAC) protocols for CR networks, considering sensing performance captured in detection and false-alarm probabilities. In particular, the contributions of this paper can be summarized as follows.

1) We design distributed synchronized MAC protocols for CR networks, incorporating spectrum-sensing operation for both single- and multiple-channel scenarios.
2) We analyze the saturation throughput of the proposed MAC protocols.
3) We perform throughput maximization of the proposed MAC protocols against their key parameters, i.e., sensing time and minimum contention window.
4) We present numerical results to illustrate performance of the proposed MAC protocols and the throughput gains due to the optimal protocol configuration.

The remainder of this paper is organized as follows. In Section II, we discuss some important related works in the literature. Section III describes the system and sensing models. The MAC protocol design, throughput analysis, and optimization for the single-channel case are performed in Section IV. The multiple-channel case is considered in Section V. Section VI presents the numerical results, followed by the concluding remarks in Section VII.

Manuscript received April 8, 2011; revised June 24, 2011; accepted August 10, 2011. Date of publication August 18, 2011; date of current version October 20, 2011. The review of this paper was coordinated by Prof. A. Jamalipour.

The authors are with the Institut National de la Recherche Scientifique—Énergie, Matériaux et Télécommunications, Université du Québec, Montréal, QC J3X 1S2, Canada (e-mail: lethanh@emt.inrs.ca; long.le@emt.inrs.ca).

Color versions of one or more of the figures in this paper are available online at http://ieeexplore.ieee.org.

Digital Object Identifier 10.1109/TVT.2011.2165325

II. Related Work

Various research problems and solution approaches have been considered for a dynamic spectrum-sharing problem in the literature. In [3] and [4], a dynamic power allocation problem for CR networks was investigated, considering fairness among SUs and interference constraints for PUs. When only mean channel gains that are averaged over short-term fading can be estimated, the authors proposed more relaxed protection constraints in terms of interference violation probabilities for the underlying fair power allocation problem. In [7], the information theory limits of CR channels were derived. A game-theoretic approach for dynamic spectrum sharing was considered in [8] and [9].

There is a rich literature on spectrum sensing for CR networks (for example, see [10] and the references therein). Classical sensing schemes based on, for example, energy detection techniques or advanced cooperative sensing strategies [11], where multiple SUs collaborate with one another to improve the sensing performance, have been investigated in the literature. There are a large number of papers that consider MAC protocol design and analysis for CR networks [12]–[19] (see [12] for a survey of recent works in this topic). However, these existing works either assumed perfect spectrum sensing or did not explicitly model the sensing imperfection in their design and analysis. In [5], the optimization of sensing and throughput tradeoff under a detection probability constraint was investigated. It was shown that the detection constraint is met with equality at optimality. However, this optimization tradeoff was only investigated for a simple scenario with one pair of SUs. The extension of this sensing and throughput tradeoff to wireless fading channels was considered in [20].

There are also some recent works that propose to exploit cooperative relays to improve the sensing and throughput performance of CR networks. In particular, a novel selective fusion spectrum-sensing and best relay data transmission scheme was proposed in [21]. A closed-form expression for the spectrum hole utilization efficiency of the proposed scheme was derived, and significant performance improvement compared with other sensing and transmission schemes was demonstrated through extensive numerical studies. In [22], a selective relay-based cooperative spectrum-sensing scheme was proposed, which does not require a separate channel for reporting sensing results. In addition, the proposed scheme can achieve excellent sensing performance with controllable interference to PUs. These existing works, however, only consider a simple setting with one pair of SUs.

III. System and Spectrum-Sensing Models

In this section, we describe the system and spectrum-sensing models. In particular, sensing performance in terms of detection and false-alarm probabilities are explicitly described.

A. System Model

We consider a network setting where N pairs of SUs opportunistically exploit available frequency bands, which belong to a primary network, for their data transmission. Note that the optimization model in [5] is a special case of our model with only one pair of SUs. In particular, we will consider both scenarios in which one or multiple radio channels are exploited by these SUs. We will design synchronized MAC protocols for both scenarios, assuming that each channel can be in the idle or busy state for a predetermined periodic interval, which is referred to as a cycle in this paper.

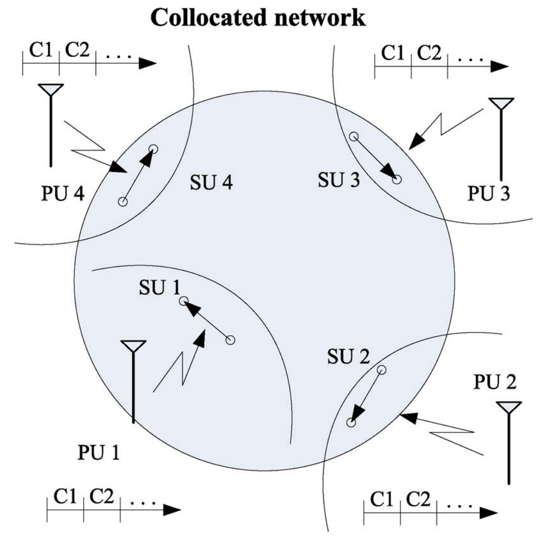

Fig. 1. Network and spectrum sharing model that was considered in this paper.

We further assume that each pair of SUs can overhear transmissions from other pairs of SUs (i.e., collocated networks). In addition, it is assumed that transmission from each individual pair of SUs affects one different primary receiver. It is straightforward to relax this assumption to the scenario where each pair of SUs affects more than one primary receiver and where each primary receiver is affected by more than one pair of SUs. The network setting under investigation is shown in Fig. 1. In the following discussion, we will interchangeably refer to pair i of SUs as secondary link i or flow i.

Remark 1: In practice, SUs can change their idle/busy status any time (i.e., status changes can occur in the middle of any cycle). Our assumption on synchronous channel status changes is only needed to estimate the system throughput. In general, imposing this assumption would not sacrifice the accuracy of our network throughput calculation if PUs maintain their idle/busy status for a sufficiently long time on the average. This is actually the case for several practical scenarios such as in TV bands, as reported by several recent studies (see [2] and the references therein). In addition, our MAC protocols that were developed under this assumption would result in very few collisions with PUs, because the cycle time is quite small compared to typical active/idle periods of PUs.

B. Spectrum Sensing

We assume that secondary links rely on a distributed synchronized MAC protocol to share available frequency channels. In particular, time is divided into fixed-size cycles, and it is assumed that secondary links can perfectly synchronize with each other (i.e., there is no synchronization error) [17], [23]. It is assumed that each secondary link performs spectrum sensing at the beginning of each cycle and only proceeds to contention with other links to transmit on available channels if its sensing outcomes indicate at least one available channel (i.e., channels that are not used by nearby PUs). For the multiple-channel case, we assume that there are M channels and each secondary transmitter is equipped with M sensors to simultaneously sense all channels. Detailed MAC protocol design will be elaborated in the following sections.

Let $\mathcal{H}_0$ and $\mathcal{H}_1$ denote the events that a particular PU is idle and active, respectively (i.e., the underlying channel is available and busy, respectively) in any cycle. In addition, let $\mathcal{P}^{ij}(\mathcal{H}_0)$ and $\mathcal{P}^{ij}(\mathcal{H}_1) = 1 - \mathcal{P}^{ij}(\mathcal{H}_0)$ be the probabilities that channel j is available and not available at secondary link i, respectively. We assume that SUs employ an energy detection scheme. Let f_s be the sampling frequency that is used in the sensing period whose length is τ for all secondary links. The following two important performance measures for quantifying the sensing performance are given as follows: 1) detection probability and 2) false-alarm probabilities. In particular, a detection event occurs when a secondary link successfully senses a busy channel, and false-alarm represents the situation when a spectrum sensor returns a busy state for an idle channel (i.e., a transmission opportunity is overlooked).

Assume that transmission signals from PUs are complex-valued phase-shift keying (PSK) signals, whereas the noise at the secondary links is independent and identically distributed circularly symmetric complex Gaussian $\mathcal{CN}(0, N_0)$ [5]. Then, the detection and false-alarm probabilities for the channel j at secondary link i can be calculated as [5]

$$\mathcal{P}_d^{ij}(\varepsilon^{ij}, \tau) = \mathcal{Q}\left(\left(\frac{\varepsilon^{ij}}{N_0} - \gamma^{ij} - 1\right)\sqrt{\frac{\tau f_s}{2\gamma^{ij}+1}}\right) \quad (1)$$

$$\begin{aligned}\mathcal{P}_f^{ij}(\varepsilon^{ij}, \tau) &= \mathcal{Q}\left(\left(\frac{\varepsilon^{ij}}{N_0} - 1\right)\sqrt{\tau f_s}\right)\\ &= \mathcal{Q}\left(\sqrt{2\gamma^{ij}+1}\,\mathcal{Q}^{-1}\left(\mathcal{P}_d^{ij}(\varepsilon^{ij}, \tau)\right) + \sqrt{\tau f_s}\gamma^{ij}\right) \quad (2)\end{aligned}$$

where $i \in [1, N]$ is the index of a SU link, $j \in [1, M]$ is the index of a channel, ε^{ij} is the detection threshold for an energy detector, γ^{ij} is the signal-to-noise ratio (SNR) of the PU's signal at the secondary link, f_s is the sampling frequency, N_0 is the noise power, τ is the sensing interval, and $\mathcal{Q}(.)$ is defined as $\mathcal{Q}(x) = (1/\sqrt{2\pi})\int_x^{\infty} \exp(-t^2/2)dt$. In the analysis performed in the following sections, we assume a homogeneous scenario where sensing performance on different channels is the same for each SU. In this case, we denote these probabilities for SU i as $\mathcal{P}_f^i$ and $\mathcal{P}_d^i$ for brevity.

Remark 2: For simplicity, we do not consider the impact of wireless channel fading in modeling the sensing performance in (1) and (2). This approach enables us to gain insight into the investigated spectrum sensing and access problem while keeping the problem sufficiently tractable. The extension of the model to capture wireless fading will be considered in our future works. Relevant results that were published in some recent works, e.g., in [20], would be useful for these further studies.

Remark 3: The analysis that was performed in the following sections can easily be extended to the case where each secondary transmitter is equipped with only one spectrum sensor or each secondary transmitter only senses a subset of all channels in each cycle. In particular, we will need to adjust the sensing time for some spectrum-sensing performance requirements. In particular, if only one spectrum sensor is available at each secondary transmitter, then the required sensing time should be M times larger than the case in which each transmitter has M spectrum sensors.

IV. Medium Access Control Design, Analysis, and Optimization: Single-Channel Case

We consider the MAC protocol design, its throughput analysis, and optimization for the single-channel case in this section.

A. MAC Protocol Design

We now describe our proposed synchronized MAC for dynamic spectrum sharing among secondary flows. We assume that each fixed-size cycle of length T is divided into the following three phases: 1) the sensing phase; 2) the synchronization phase; and 3) the data transmission phase. During the sensing phase of length τ, all SUs perform spectrum sensing on the underlying channel. Then, only secondary links whose sensing outcomes indicate an available channel proceed to the next phase (they will be called active SUs or secondary links in the following discussion). In the synchronization phase, active SUs broadcast beacon signals for synchronization. Finally, active SUs perform contention and transmit data in the data transmission phase. The timing diagram of one particular cycle is illustrated in Fig. 2. For this single-channel scenario, synchronization, contention, and data transmission occur on the same channel.

We assume that the length of each cycle is sufficiently large so that secondary links can transmit several packets during the data transmission phase. Indeed, the current IEEE 802.22 standard specifies that the spectrum evacuation time upon the return of PUs is 2 s, which is a relatively large interval. Therefore, our assumption would be valid for most practical cognitive systems. During the data transmission phase, we assume that active secondary links employ a standard contention technique to capture the channel similar to the carrier sense multiple access with collision avoidance (CSMA/CA) protocol. Exponential backoff with minimum contention window W and maximum backoff stage m [24] is employed in the contention phase. For brevity, we simply refer to W as the contention window in the following discussion. In particular, suppose that the current backoff stage of a particular SU is i. Then, it starts the contention by choosing a random backoff time uniformly distributed in the range $[0, 2^i W - 1]$, $0 \le i \le m$. This user then starts decrementing its backoff time counter while carrier sensing transmissions from other secondary links.

Let σ denote a minislot interval, each of which corresponds one unit of the backoff time counter. Upon hearing a transmission from any secondary link, each secondary link will "freeze" its backoff time counter and reactivate when the channel is again sensed idle. Otherwise, if the backoff

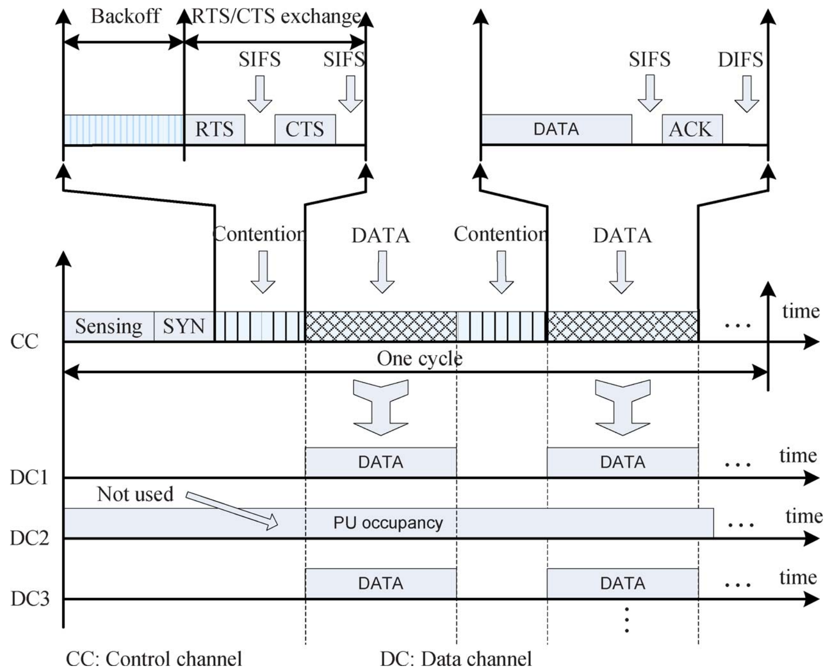

Fig. 2. Timing diagram of the proposed multiple-channel MAC protocol.

time counter reaches zero, the underlying secondary link wins the contention. Here, either two- or four-way handshake with request to send/clear to send (RTS/CTS) will be employed to transmit one data packet on the available channel. In the four-way handshake, the transmitter sends RTS to the receiver and waits until it successfully receives CTS before sending a data packet. In both handshake schemes, after sending the data packet, the transmitter expects an acknowledgment (ACK) from the receiver to indicate a successful reception of the packet. Standard small intervals, i.e., distributed interframe space (DIFS) and short interframe space (SIFS), are used before backoff time decrements and ACK packet transmission, as described in [24]. We refer to this two-way handshaking technique as the basic access scheme in the following analysis.

B. Throughput Maximization

Given the sensing model and proposed MAC protocol, we are interested in finding its optimal configuration to achieve the maximum throughput subject to protection constraints for primary receivers. In particular, let $\mathcal{NT}(\tau, W)$ be the normalized total throughput, which is a function of sensing time τ and contention window W. Suppose that each primary receiver requires that the detection probability that is achieved by its conflicting primary link i is at least $\overline{P}_d^i$. Then, the throughput maximization problem can be stated as follows:

Problem 1: We have

$$\begin{aligned} &\max_{\tau, W} \quad \mathcal{NT}(\tau, W) \\ &\text{s.t.} \quad \mathcal{P}_d^i(\varepsilon^i, \tau) \geq \bar{\mathcal{P}}_d^i, \quad i = 1, 2, \cdots, N \\ &\qquad 0 < \tau \leq T, \quad 0 < W \leq W_{\mathsf{max}} \end{aligned} \tag{3}$$

where W_{max} is the maximum contention window. Recall that T is the cycle interval. In fact, optimal sensing τ would allocate sufficient time to protect primary receivers, and the optimal contention window would balance between reducing collisions among active secondary links and limiting the protocol overhead.

C. Throughput Analysis and Optimization

We perform saturation throughput analysis and solve the optimization problem (3) in this section. The throughput analysis for the CR setting under investigation is more involved compared to the standard MAC protocol throughput analysis (for example, see [23] and [24]), because the number of active secondary links that participate in the contention in each cycle varies, depending on the sensing outcomes. Suppose that all secondary links have the same packet length. Let $\Pr(n = n_0)$ and $\mathcal{T}(\tau, \phi | n = n_0)$ be the probability that n_0 secondary links participate in the contention and the conditional normalized throughput when n_0 secondary links join the channel contention, respectively. Then, the normalized throughput can be calculated as

$$\mathcal{NT} = \sum_{n_0=1}^{N} \mathcal{T}(\tau, W | n = n_0) \Pr(n = n_0) \tag{4}$$

where, as aforementioned, N is the number of secondary links, τ is the sensing time, and W is the contention window. In the following discussion, we show how we can calculate $\Pr(n = n_0)$ and $\mathcal{T}(\tau, \phi | n = n_0)$.

1) Calculation of $\Pr(n = n_0)$*:* Note that only secondary links whose sensing outcomes in the sensing phase indicate an available channel proceed to contention in the data transmission phase. This case can happen for a particular secondary link i in the following two scenarios.

- The PU is not active, and no false alarm is generated by the underlying secondary link.
- The PU is active, and secondary link i misdetects its presence.

Therefore, secondary link i joins contention in the data transmission phase with probability

$$\mathcal{P}_{idle}^{i} = \left[1 - \mathcal{P}_{f}^{i}(\varepsilon^{i}, \tau)\right] \mathcal{P}^{i}(\mathcal{H}_{0}) + \mathcal{P}_{m}^{i}(\varepsilon^{i}, \tau)\mathcal{P}^{i}(\mathcal{H}_{1}) \quad (5)$$

where $\mathcal{P}_{m}^{i}(\varepsilon^{i}, \tau) = 1 - \mathcal{P}_{d}^{i}(\varepsilon^{i}, \tau)$ is the misdetection probability. Otherwise, it will be silent for the whole cycle and waits until the next cycle. This case occurs with probability

$$\begin{aligned}\mathcal{P}_{busy}^{i} &= 1 - \mathcal{P}_{idle}^{i} \\ &= \mathcal{P}_{f}^{i}(\varepsilon^{i}, \tau)\mathcal{P}^{i}(\mathcal{H}_{0}) + \mathcal{P}_{d}^{i}(\varepsilon^{i}, \tau)\mathcal{P}^{i}(\mathcal{H}_{1}). \quad (6)\end{aligned}$$

We assume that the interference of active PUs to the SU is negligible; therefore, a transmission from any secondary link fails only when it collides with transmissions from other secondary links. Now, let $\mathcal{S}_k$ denote one particular subset of all secondary links with exactly n_0 secondary links. There are $C_N^{n_0} = N!/n_0!(N - n_0)!$ such sets $\mathcal{S}_k$. The probability of the event that n_0 secondary links join contention in the data transmission phase can be calculated as

$$\Pr(n = n_0) = \sum_{k=1}^{C_N^{n_0}} \prod_{i \in \mathcal{S}_k} \mathcal{P}_{idle}^{i} \prod_{j \in \mathcal{S}\backslash\mathcal{S}_k} \mathcal{P}_{busy}^{j} \quad (7)$$

where $\mathcal{S}$ denotes the set of all N secondary links, and $\mathcal{S}\backslash\mathcal{S}_k$ is the complement of $\mathcal{S}_k$ with $N - n_0$ secondary links. If all secondary links have the same SNR_p and the same probabilities $\mathcal{P}^i(\mathcal{H}_0)$ and $\mathcal{P}^i(\mathcal{H}_1)$, then we have $\mathcal{P}_{idle}^{i} = \mathcal{P}_{idle}$ and $\mathcal{P}_{busy}^{i} = \mathcal{P}_{busy} = 1 - \mathcal{P}_{idle}$ for all i. In this case, (7) becomes

$$\Pr(n = n_0) = C_N^{n_0}(1 - \mathcal{P}_{busy})^{n_0}(\mathcal{P}_{busy})^{N-n_0} \quad (8)$$

where all terms in the sum of (7) become the same.

Remark 4: In general, interference from active PUs will impact transmissions of SUs. However, strong interference from PUs would imply a high SNR of sensing signals that were collected at PUs. In this high-SNR regime, we typically require small sensing time while still satisfactorily protecting PUs. Therefore, for the case in which interference from active PUs to SUs is small, the sensing time will have the most significant impact on the investigated sensing-throughput tradeoff. Therefore, considering this setting enables us to gain better insight into the underlying problem. Extension to the more general case is possible by explicitly calculating the transmission rates that are achieved by SUs as a function of the signal-to-inference-plus-noise ratio (SINR). Due to space constraints, we will not further explore this issue in this paper.

2) Calculation of the Conditional Throughput: The conditional throughput can be calculated using the technique that was developed by Bianchi in [24], where we approximately assume a fixed transmission probability ϕ in a generic slot time. In particular, Bianchi shows that this transmission probability can be calculated from the following two equations [24]:

$$\phi = \frac{2(1 - 2p)}{(1 - 2p)(W + 1) + Wp\left(1 - (2p)^m\right)} \quad (9)$$

$$p = 1 - (1 - \phi)^{n-1} \quad (10)$$

where m is the maximum backoff stage, and p is the conditional collision probability (i.e., the probability that a collision is observed when a data packet is transmitted on the channel).

Supposing that there are n_0 secondary links that participate in contention in the third phase, the probability of the event that at least one secondary link transmits its data packet can be written as

$$\mathcal{P}_t = 1 - (1 - \phi)^{n_0}. \quad (11)$$

However, the probability that a transmission occurs on the channel is successful, given that there is at least one secondary link that transmits, can be written as

$$\mathcal{P}_s = \frac{n_0\phi(1 - \phi)^{n_0 - 1}}{\mathcal{P}_t}. \quad (12)$$

The average duration of a generic slot time can be calculated as

$$\bar{T}_{sd} = (1 - \mathcal{P}_t)T_e + \mathcal{P}_t\mathcal{P}_sT_s + \mathcal{P}_t(1 - \mathcal{P}_s)T_c \quad (13)$$

where $T_e = \sigma$, T_s, and T_c represent the duration of an empty slot, the average time that the channel is sensed busy due to a successful transmission, and the average time that the channel is sensed busy due to a collision, respectively. These quantities can be calculated as follows [24]:

For the basic mechanism, we have

$$\begin{cases} T_s = T_s^1 = H + PS + SIFS + 2PD + ACK + DIFS \\ T_c = T_c^1 = H + PS + DIFS + PD \\ H = H_{PHY} + H_{MAC} \end{cases} \quad (14)$$

where H_{PHY} and H_{MAC} are the packet headers for the physical and MAC layers, PS is the packet size, which is assumed to be fixed in this paper, PD is the propagation delay, $SIFS$ is the length of a SIFS, $DIFS$ is the length of a DIFS, and ACK is the length of an ACK.

For the RTS/CTS mechanism, we have

$$\begin{cases} T_s = T_s^2 = H + PS + 3SIFS + 2PD \\ \quad +RTS + CTS + ACK + DIFS \\ T_c = T_c^2 = H + DIFS + RTS + PD \end{cases} \quad (15)$$

where we abuse the notations by letting RTS and CTS represent the length of RTS and CTS control packets, respectively.

Based on these quantities, we can express the conditional normalized throughput as follows:

$$\mathcal{T}(\tau, \phi | n = n_0) = \left\lfloor \frac{T - \tau}{\bar{T}_{sd}} \right\rfloor \frac{\mathcal{P}_s\mathcal{P}_tPS}{T} \quad (16)$$

where $\lfloor . \rfloor$ denotes the floor function, and T is the duration of a cycle. Note that $\lfloor T - \tau/\bar{T}_{sd} \rfloor$ denotes the average number of generic slot times in one particular cycle, excluding the sensing phase. Here, we omit the length of the synchronization phase, which is assumed to be negligible.

3) Optimal Sensing and the MAC Protocol Design: Now, we turn to solve the throughput maximization problem that was formulated in (3). Note that we can calculate the normalized throughput, as given by (4), by using $\Pr(n = n_0)$, which is calculated from (7), and the conditional throughput, which is calculated from (16). It can be observed that the detection probability $\mathcal{P}_d^i(\varepsilon^i, \tau)$ in the primary protection constraints $\mathcal{P}_d^i(\varepsilon^i, \tau) \geq \bar{\mathcal{P}}_d^i$ depends on both the detection threshold ε^i and the optimization variable τ.

We can show that, by optimizing the normalized throughput over τ and W while fixing detection thresholds $\varepsilon^i = \varepsilon_0^i$, where $\mathcal{P}_d^i(\varepsilon_0^i, \tau) = \bar{\mathcal{P}}_d^i$, $i = 1, 2, \ldots, N$, we can achieve the almost-maximum throughput gain. The intuition behind this observation can be interpreted as follows. If we choose $\varepsilon^i < \varepsilon_0^i$ for a given τ, then both $\mathcal{P}_d^i(\varepsilon^i, \tau)$ and $\mathcal{P}_f^i(\varepsilon^i, \tau)$ increase compared to the case $\varepsilon^i = \varepsilon_0^i$. As a result, $\mathcal{P}_{busy}^i$, as given in (6), increases. Moreover, it can be verified that the increase in $\mathcal{P}_{busy}^i$ will lead to the shift of the probability distribution $\Pr(n = n_0)$ to the left. In particular, $\Pr(n = n_0)$, as given in (7), increases for small n_0 and decreases for large n_0 as $\mathcal{P}_{busy}^i$ increases. Fortunately, with an appropriate choice of contention window W, the conditional throughput $\mathcal{T}(\tau, W|n = n_0)$, as given in (16), is quite flat for different n_0 (i.e., it only slightly decreases when n_0 increases). Therefore, the normalized throughput, as given by (4), is almost a constant when we choose $\varepsilon^i < \varepsilon_0^i$.

In the following discussion, we will optimize the normalized throughput over τ and W while choosing detection thresholds such that $\mathcal{P}_d^i(\varepsilon_0^i, \tau) = \bar{\mathcal{P}}_d^i$, $i = 1, 2, \ldots, N$. Based on these equality constraints and (2), we have

$$\mathcal{P}_f^i = \mathcal{Q}(\alpha^i + \sqrt{\tau f_s}\gamma^i) \tag{17}$$

where $\alpha^i = \sqrt{2\gamma^i + 1}\mathcal{Q}^{-1}(\bar{\mathcal{P}}_d^i)$. Hence, the optimization problem (3) becomes independent of all detection thresholds ε^i, $i = 1, 2, \ldots, N$. Unfortunately, this optimization problem is still a mixed integer program (note that W takes integer values), which is difficult to solve. In fact, it can be verified that, even if we allow W to be a real number, the resulting optimization problem is still not convex, because the objective function is not concave [27]. Therefore, standard convex optimization techniques cannot be employed to find the optimal solution for the optimization problem under investigation. Therefore, we have to rely on numerical optimization [25] to find the optimal configuration for the proposed MAC protocol. In particular, for a given contention window W, we can find the corresponding optimal sensing time τ as follows.

Problem 2: We have

$$\max_{0<\tau\leq T} \mathcal{NT}(\tau, W) = \sum_{n_0=1}^{N} \mathcal{T}(\tau, W|n=n_0) \Pr(n=n_0). \tag{18}$$

This optimization problem is not convex, because its objective function is not concave in general. However, we will prove that $\mathcal{NT}(\tau)$ is a unimodal function in the range of $[0, T]$. In particular, $\mathcal{NT}(\tau)$ is monotonically increasing in $[0, \bar{\tau})$, whereas it is monotonically decreasing in $(\bar{\tau}, T]$ for some $0 < \bar{\tau} \leq T$. Hence, $\mathcal{NT}(\bar{\tau})$ is the only global maximum in the entire range of $[0, T]$. This property is formally stated in the following proposition.

Proposition 1: The objective function $\mathcal{NT}(\tau)$ of (18) satisfies the following properties.

1) $\lim_{\tau\to T}(\partial\mathcal{NT}/\partial\tau) < 0$.
2) $\lim_{\tau\to 0}(\partial\mathcal{NT}/\partial\tau) = +\infty$.
3) There is a unique $\bar{\tau}$, where $\bar{\tau}$ is in the range of $[0, T]$ such that $\partial\mathcal{NT}(\bar{\tau})/\partial\tau = 0$.
4) The objective function $\mathcal{NT}(\tau)$ is bounded from above.

Proof: The proof is provided in Appendix A. ■

We would like to discuss the properties that were stated in Proposition 1. Properties 1, 2, and 4 imply that there must be at least one τ in $[0, T]$ that maximizes $\mathcal{NT}(\tau)$. The second property implies that, indeed, such an optimal solution is unique. Therefore, we can find the globally optimal (W^*, τ^*) by finding optimal τ for each W in its feasible range $[1, W_{\max}]$. The procedure for finding (W^*, τ^*) can be described in Algorithm 1. Numerical studies reveal that this algorithm has quite-low computation time for practical values of $W_{\max}$ and T.

Algorithm 1: OPTIMIZATION OF THE COGNITIVE MAC PROTOCOL.

1: For each integer value of $W \in [1, W_{\max}]$, find the optimal τ according to (18), i.e.,

$$\bar{\tau}(W) = \underset{0<\tau\leq T}{\arg\max} \quad \mathcal{NT}(\tau, W). \tag{19}$$

2: The globally optimal (W^*, τ^*) can then be found as

$$(W^*, \tau^*) = \underset{W, \bar{\tau}(W)}{\arg\max} \quad \mathcal{NT}\left(\bar{\tau}(W), W\right). \tag{20}$$

D. Some Practical Implementation Issues

Implementation for the proposed optimal MAC protocol configuration can be done as follows. Each SU will need to spend some time to estimate the channel availability probabilities, channel SNRs, and the number of SUs that share the underlying spectrum. When these system parameters have been estimated, each SU can independently calculate the optimal sensing time and minimum contention window and implement them. Therefore, implementation for the optimal MAC protocol can be performed in a completely distributed manner, which would be very desirable.

V. MEDIUM ACCESS CONTROL DESIGN, ANALYSIS, AND OPTIMIZATION: MULTIPLE-CHANNEL CASE

We consider the MAC protocol design, analysis, and optimization for the multiple-channel case in this section.

A. MAC Protocol Design

We propose a synchronized multichannel MAC protocol for dynamic spectrum sharing in this section. To exploit spectrum holes in this case, we assume that there is one control channel that belongs to the secondary network (i.e., it is always available) and M data channels that can be exploited by SUs. We further assume that each transmitting SU employs a reconfigurable transceiver that can easily be tuned to the control channel or vacant channels for data transmission. In addition, we assume that this transceiver can turn on and off the carriers on the available or busy channels, respectively; for example, this approach can be achieved by the orthogonal frequency-division multiplexing (OFDM) technology.

There are still three phases for each cycle as in the single-channel case. However, in the first phase, i.e., the sensing phase of length τ, all SUs simultaneously perform spectrum sensing on all M underlying channels. Because the control channel is always available, all SUs exchange beacon signals to achieve synchronization in the second phase. Moreover, only active secondary links whose sensing outcomes indicate at least one vacant channel participate in the third phase (i.e., the data transmission phase). As a result, the transmitter of the winning link in the contention phase will need to inform its receiver about the available channels. Finally, the winning secondary link will transmit data on all vacant channels in the data transmission phase. The timing diagram of one particular cycle is illustrated in Fig. 2.

Again, we assume that the length of each cycle is sufficiently large such that secondary links can transmit several packets on each available channel during the data transmission phase. In the data transmission phase, we assume that active secondary links adopt the standard contention technique to capture the channels similar to the approach employed by the CSMA/CA protocol using exponential backoff and either two- or four-way handshake, as described in Section III. For the case with two-way handshake, both secondary transmitters and receivers need to perform spectrum sensing. With four-way handshake, only secondary transmitters need to perform spectrum sensing, and the RTS message will contain additional information about the available channels on which the receiver will receive data packets. In addition, multiple packets (i.e., one on each available channel) are transmitted by the winning secondary transmitter. Finally, the ACK message will be sent by the receiver to indicate successfully received packets on the vacant channels.

B. Throughput Maximization

In this section, we discuss how we can find the optimal configuration to maximize the normalized throughput under sensing constraints for PUs. Suppose that each primary receiver requires that the detection probability that is achieved by its conflicting primary link i on channel j is at least $\overline{P}_d^{ij}$. Then, the throughput maximization problem can be stated as follows.

Problem 3: We have

$$\begin{aligned} \max_{\tau,W} \quad & \mathcal{NT}(\tau, W) \\ \text{s.t.} \quad & \mathcal{P}_d^{ij}(\varepsilon^{ij}, \tau) \geq \bar{\mathcal{P}}_d^{ij}, i \in [1, N], j \in [1, M] \\ & 0 < \tau \leq T, 0 < W \leq W_{\mathsf{max}} \end{aligned} \tag{21}$$

where $\mathcal{P}_d^{ij}$ is the detection probability for SU i on channel j, W_{max} is the maximum contention window, and T is the cycle interval. We will assume that, for each SU i, $\mathcal{P}_d(\varepsilon^{ij}, \tau)$, and $\bar{\mathcal{P}}_d^{ij}$ are the same for all channels j, respectively. This condition would be valid, because the sensing performance (i.e., captured in $\mathcal{P}_d(\varepsilon^{ij}, \tau)$ and $\mathcal{P}_f(\varepsilon^{ij}, \tau)$) depends on the detection thresholds ϵ^{ij} and the SNR γ^{ij}, which would be the same for different channels j. In this case, the optimization problem reduces to the same form as in (3), although the normalized throughput $\mathcal{NT}(\tau, W)$ will need to be derived for this multiple-channel case. For brevity, we will drop all channel indices j in these quantities whenever possible.

C. Throughput Analysis and Optimization

We analyze the saturation throughput and show how we can obtain an optimal solution for *Problem 3*. Again, we assume that all secondary links transmit data packets of the same length. Let $\Pr(n = n_0)$, $\mathbf{E}[l]$, and $\mathcal{T}(\tau, \phi | n = n_0)$ denote the probability that n_0 secondary links participate in the contention phase, the average number of vacant channels at the winning SU link, and the conditional normalized throughput when n_0 secondary links join the contention, respectively. Then, the normalized throughput can be calculated as

$$\mathcal{NT} = \sum_{n_0=1}^{N} \mathcal{T}(\tau, W | n = n_0) \Pr(n = n_0) \frac{\mathbf{E}[l]}{M} \tag{22}$$

where N is the number of secondary links, M is the number of channels, τ is the sensing time, and W is the contention window. Note that this value is the average system throughput per channel. We will calculate $\mathcal{T}(\tau, \phi | n = n_0)$ using (16) for the proposed MAC protocol with four-way handshake and exponential random backoff. In addition, we show how we can calculate $\Pr(n = n_0)$.

1) Calculation of $\Pr(n = n_0)$ *and* $\mathbf{E}[l]$*:* Recall that only secondary links whose sensing outcomes indicate at least one available channel participate in contention in the data transmission phase. Again, similar to the single-channel case that was derived in Section IV-C1, the sensing outcome at SU i indicates that channel j is available or busy with probabilities $\mathcal{P}_{idle}^i$ and $\mathcal{P}_{busy}^i$, which are in the same form with (5) and (6), respectively (recall that we have dropped the channel index j in these quantities). Now, $\Pr(n = n_0)$ can be calculated from these probabilities. Recall that secondary link i joins the contention only if its sensing outcomes indicate at least one vacant channel. Otherwise, it will be silent for the whole cycle and waits until the next cycle. This case occurs if its sensing outcomes indicate that all channels are busy.

To gain insight into the optimal structure of the optimal solution while keeping mathematical details sufficiently tractable, we will consider the homogeneous case in the following discussion, where $\mathcal{P}_f^i$, $\mathcal{P}_d^i$ (therefore, $\mathcal{P}_{idle}^i$ and $\mathcal{P}_{busy}^i$) are the same for all SUs i. The obtained results, however, can be extended to the general case, although the corresponding expressions will be more lengthy and tedious. For the homogeneous system, we will simplify $\mathcal{P}_{SUidle}^i$ and $\mathcal{P}_{SUbusy}^i$ to $\mathcal{P}_{SUidle}$ and $\mathcal{P}_{SUbusy}$, respectively, for brevity. Therefore, the probability that a particular channel is indicated as busy or idle by the corresponding spectrum sensor can be written as

$$\mathcal{P}_{busy} = \mathcal{P}_f \mathcal{P}(\mathcal{H}_0) + \mathcal{P}_d \mathcal{P}(\mathcal{H}_1) \tag{23}$$

$$\mathcal{P}_{idle} = 1 - \mathcal{P}_{busy}. \tag{24}$$

Let $Pr(l = l_0)$ denote the probability that l_0 out of M channels are indicated as available by the spectrum sensors. Then, this probability can be calculated as

$$\Pr(l = l_0) = C_M^{l_0} \mathcal{P}_{idle}^{l_0} \mathcal{P}_{busy}^{M-l_0}. \tag{25}$$

Now, let $\mathcal{P}_{SUidle}$ be the probability that a particular secondary link i participates in the contention (i.e., its spectrum sensors indicate at least one available channel) and $\mathcal{P}_{SUbusy}$ be the probability that secondary link i is silent (i.e., its spectrum sensors indicate that all channels are busy). Then, these probabilities can be calculated as

$$\mathcal{P}_{SUbusy} = \Pr(l=0) = \mathcal{P}_{busy}^{M} \tag{26}$$

$$\mathcal{P}_{SUidle} = \sum_{l_0=1}^{M} \Pr(l=l_0) = 1 - \mathcal{P}_{SUbusy}. \tag{27}$$

Again, we assume that a transmission from a particular secondary link fails only if it collides with transmissions from other secondary links. The probability that n_0 secondary links join the contention can be calculated using (26) and (27) as follows:

$$\begin{aligned}\Pr(n=n_0) &= C_N^{n_0} \mathcal{P}_{SUidle}^{n_0} \mathcal{P}_{SUbusy}^{N-n_0} \\ &= C_N^{n_0}\left(1-\mathcal{P}_{busy}^{M}\right)^{n_0} \mathcal{P}_{busy}^{M(N-n_0)}.\end{aligned} \tag{28}$$

Based on (25), we can calculate the average number of available channels, which is denoted by the expectation $\mathbf{E}[l]$, at one particular secondary link as

$$\begin{aligned}\mathbf{E}[l] &= \sum_{l_0=0}^{M} l_0 \Pr(l=l_0) = \sum_{l_0=0}^{M} l_0 C_M^{l_0} \mathcal{P}_{idle}^{l_0} \mathcal{P}_{busy}^{M-l_0} \\ &= M\mathcal{P}_{idle} = M(1-\mathcal{P}_{busy}).\end{aligned} \tag{29}$$

2) Optimal Sensing and the MAC Protocol Design: We now tackle the throughput maximization problem that was formulated in (21). In this case, the normalized throughput, as given by (22), can be calculated using $\Pr(n=n_0)$ in (28), the conditional throughput in (16), and the average number of available channels in (29). Similar to the single-channel case, we will optimize the normalized throughput over τ and W while choosing a detection threshold such that $\mathcal{P}_d(\varepsilon_0, \tau) = \bar{\mathcal{P}}_d$. Under these equality constraints, the false-alarm probability can be written as

$$\mathcal{P}_f = \mathcal{Q}(\alpha + \sqrt{\tau f_s}\gamma) \tag{30}$$

where $\alpha = \sqrt{2\gamma+1}\mathcal{Q}^{-1}(\bar{\mathcal{P}}_d)$. Hence, *Problem 3* is independent of detection thresholds. Again, for a given contention window W, we can find the corresponding optimal sensing time τ in the following optimization problem.

Problem 4: We have

$$\max_{\tau} \; \widetilde{\mathcal{NT}}(\tau) \triangleq NT(\tau, W)|_{W=\bar{W}} \quad s.t. \quad 0 \le \tau \le T. \tag{31}$$

Similar to the single-channel case, we will prove that $\widetilde{\mathcal{NT}}(\tau)$ is a unimodal function in the range of $[0, T]$. Therefore, there is a unique global maximum in the entire range of $[0, T]$. This case is, indeed, the result of several properties as stated in the following proposition.

Proposition 2: The function $\widetilde{\mathcal{NT}}(\tau)$ satisfies the following properties.

1) $\lim_{\tau \to 0}(\partial \widetilde{\mathcal{NT}}(\tau)/\partial \tau) > 0$.
2) $\lim_{\tau \to T}(\partial \widetilde{\mathcal{NT}}(\tau)/\partial \tau) < 0$.
3) There is a unique $\overline{\tau}$, where $\overline{\tau}$ is in the range of $[0, T]$ such that $\partial \widetilde{\mathcal{NT}}(\overline{\tau})/\partial \tau = 0$.
4) The objective function $\widetilde{\mathcal{NT}}(\tau)$ is bounded from above.

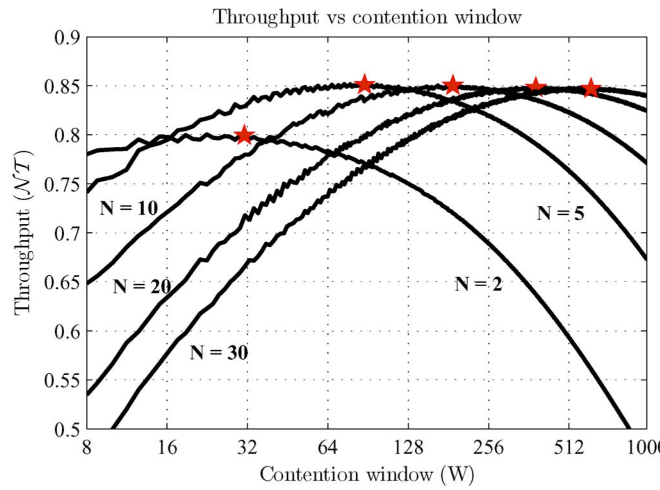

Fig. 3. Normalized throughput versus contention window W for $\tau = 1$ ms, $m = 3$, different N, and the basic access mechanism.

Therefore, it is a unimodal function in the range of $[0, T]$.

Proof: The proof is provided in Appendix B. ■

Therefore, given one particular value of W, we can find a unique optimal $\overline{\tau}(W)$ for the optimization problem (31). Then, we can find the globally optimal (W^*, τ^*) by finding optimal τ for each W in its feasible range $[1, W_{\mathbf{max}}]$. The procedure for finding (W^*, τ^*) is the same as described in **Algorithm 1**.

VI. Numerical Results

We present numerical results to illustrate the throughput performance of the proposed cognitive MAC protocols. We take key parameters for the MAC protocols from [24, Tab. II]. Other parameters are chosen as follows.

1) The cycle time is $T = 100$ ms.
2) The minislot (i.e., the generic empty slot time) is $\sigma = 20\ \mu$s.
3) The sampling frequency for spectrum sensing is $f_s = 6$ MHz.
4) The bandwidth of the PUs' quadrature phase-shift keying (QPSK) signals is 6 MHz.

In addition, the exponential backoff mechanism with the maximum backoff stage m is employed to reduce collisions.

A. Performance of the Single-Channel MAC Protocol

For the results in this section, we choose other parameters of the cognitive network as follows. The SNR of PU signals at secondary links SNR_p^i are randomly chosen in the range $[-15, -20]$ dB. The target detection probability for secondary links and the probabilities $\mathcal{P}^i(\mathcal{H}_0)$ are randomly chosen in the intervals [0.7, 0.9] and [0.7, 0.8], respectively. The basic scheme is used as a handshake mechanism for the MAC protocol.

In Fig. 3, we show the normalized throughput $\mathcal{NT}$ versus contention window W for different values of N when the sensing time is fixed at $\tau = 1$ ms and the maximum backoff stage is chosen at $m = 3$ for one particular realization of system parameters. The maximum throughput on each curve

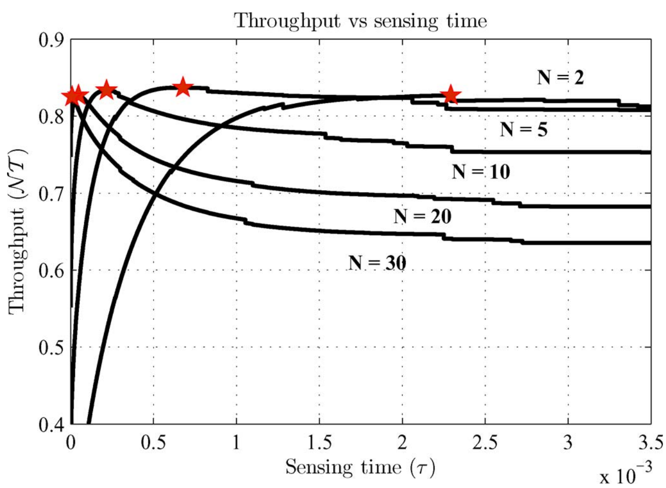

Fig. 4. Normalized throughput versus sensing time τ for $W = 32$, $m = 3$, different N, and the basic access mechanism.

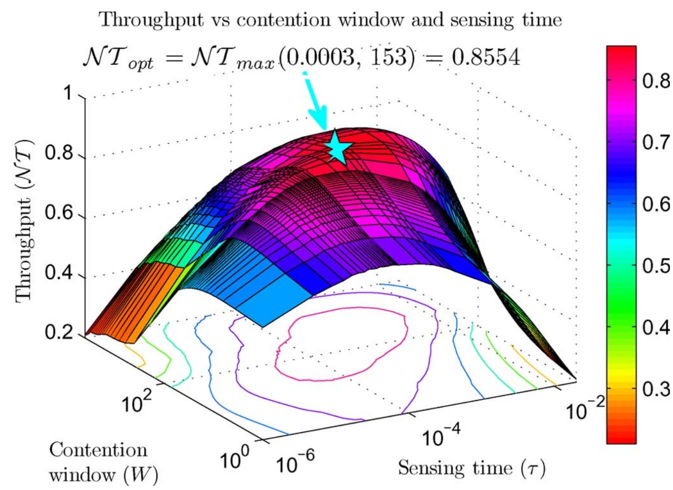

Fig. 5. Normalized throughput versus sensing time τ and contention window W for $N = 15$, $m = 4$, and the basic access mechanism.

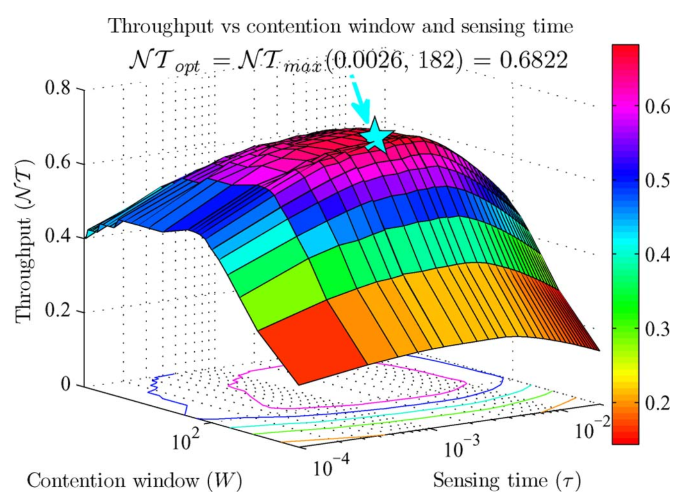

Fig. 6. Normalized throughput versus sensing time τ and contention window W for $N = 10$, $m = 4$, $M = 5$, and the basic access mechanism.

is indicated by a star symbol. This figure indicates that the maximum throughput is achieved at larger W for larger N. This case is expected, because a larger contention window can alleviate collisions among active secondary for a larger number of secondary links. It is interesting to observe that the maximum throughput can be larger than 0.8, although $\mathcal{P}^i(\mathcal{H}_0)$ are chosen in the range [0.7, 0.8]. This case is due to a multiuser gain, because secondary links are in conflict with different primary receivers.

In Fig. 4, we present the normalized throughput $\mathcal{NT}$ versus sensing time τ for a fixed contention window $W = 32$, the maximum backoff stage $m = 3$, and a different number of secondary links N. The maximum throughput is indicated by a star symbol on each curve. This figure confirms that the normalized throughput $\mathcal{NT}$ increases when τ is small and decreases with large τ, as proved in Proposition 1. Moreover, for a fixed contention window, the optimal sensing time, indeed, decreases with the number of secondary links N. Finally, the multiuser diversity gain can also be observed in this figure.

To illustrate the joint effects of contention window W and sensing time τ, we show the normalized throughput $\mathcal{NT}$ versus τ and contention window W for $N = 15$ and $m = 4$ in Fig. 5. We show the globally optimal parameters (ϕ^*, τ^*), which maximize the normalized throughput $\mathcal{NT}$ of the proposed cognitive MAC protocol, by a star symbol in this figure. Fig. 5 also reveals that the performance gain due to the optimal configuration of the proposed MAC protocol is very significant. In particular, although the normalized throughput $\mathcal{NT}$ tends to be less sensitive to the contention window W, it significantly decreases when the sensing time τ deviates from the optimal value τ^*. Therefore, the proposed optimization approach would be very useful in achieving the largest throughput performance for the secondary network.

B. Performance of the Multiple-Channel MAC Protocol

In this section, we present numerical results for the proposed multiple-channel MAC protocol. Although, we analyze the homogeneous scenario in Section V for brevity, we present simulation results for the heterogeneous settings in this section. The same parameters for the MAC protocol as in Section VI-A are used. However, this model covers for the case in which each secondary link has multiple channels. In addition, some key parameters are chosen as follows. The SNRs of the signals from the PU to secondary link i (i.e., SNR_p^{ij}) are randomly chosen in the range of $[-15, -20]$ dB. The target detection probabilities $\bar{\mathcal{P}}_d^{ij}$ and the probabilities $\mathcal{P}^{ij}(\mathcal{H}_0)$ for channel j at secondary link i are randomly chosen in the intervals [0.7, 0.9] and [0.7, 0.8], respectively. Again, the exponential backoff mechanism with the maximum backoff stage m is employed to reduce collisions.

In Fig. 6, we illustrate the normalized throughput $\mathcal{NT}$ versus sensing times τ and contention windows W for $N = 10$, $M = 5$, and $m = 4$ and the basic access mechanism. We show the optimal configuration (τ^*, W^*), which maximizes the normalized throughput $\mathcal{NT}$ of the proposed multichannel MAC protocol. Again, it can be observed that the normalized throughput $\mathcal{NT}$ tends to be less sensitive to the contention window W, whereas it significantly decreases when the sensing time τ deviates from the optimal sensing time τ^*.

TABLE I
COMPARISON BETWEEN THE NORMALIZED THROUGHPUTS OF THE BASIC AND RTS/CTS ACCESS SCHEMES

BASIC ACCESS (N,M,m) = (10,5,4)

$\mathcal{NT}$		$\tau(ms)$ 1	2.6	10	20
W	16	0.4865	0.5545	0.5123	0.4677
	64	0.5803	0.6488	0.6004	0.5366
	182	0.6053	**0.6822**	0.6323	0.5594
	512	0.6014	0.6736	0.6251	0.5567
	1024	0.5744	0.6449	0.5982	0.5312

RTS/CTS ACCESS (N,M,m) = (10,5,4)

$\mathcal{NT}$		$\tau(ms)$ 1	2.6	10	20
W	16	0.6029	0.6654	0.6236	0.5568
	60	0.6022	**0.6733**	0.6231	0.5568
	128	0.5954	0.6707	0.6175	0.5533
	512	0.5737	0.6444	0.5982	0.5323
	1024	0.5468	0.6134	0.5692	0.5059

BASIC ACCESS (N,M,m) = (5,3,4)

$\mathcal{NT}$		$\tau(ms)$ 1	2.3	10	20
W	16	0.5442	0.6172	0.5647	0.5079
	64	0.6015	0.6757	0.6302	0.5565
	100	0.6094	**0.6841**	0.6345	0.5665
	512	0.5735	0.6443	0.5983	0.5324
	1024	0.5210	0.5866	0.5447	0.4842

RTS/CTS ACCESS (N,M,m) = (5,3,4)

$\mathcal{NT}$		$\tau(ms)$ 1	2.5	10	20
W	22	0.5972	**0.6789**	0.6177	0.5529
	64	0.5931	0.6674	0.6217	0.5483
	128	0.5876	0.6604	0.6131	0.5441
	512	0.5458	0.6128	0.5691	0.5057
	1024	0.4965	0.5591	0.5189	0.4610

To study the joint effect of contention window W and sensing time τ in greater detail, we show the normalized throughput $\mathcal{NT}$ versus W and τ in Table I. In this table, we consider both handshake mechanisms, i.e., the basic and RTS/CTS access schemes. Each set of results applies to a particular setting with a certain number of secondary links N, a number of channels M, and the maximum backoff stage m. In particular, we will consider the following two settings: 1) $(N, M, m) = (10, 5, 4)$, and 2) $(N, M, m) = (5, 3, 5)$. The optimal normalized throughput is indicated by a bold number. It can be confirmed from this table that, as (τ, W) deviates from the optimal (τ^*, W^*), the normalized throughput significantly decreases.

This table also demonstrates potential effects of the number of secondary links N on the network throughput and optimal configuration for the MAC protocols. In particular, for secondary networks with a small number of secondary links, the probability of collision is lower than for networks with a large number of secondary links. We consider the two scenarios that correspond to different combinations (N, M, m). The first scenario, which has a smaller number of secondary links N, indeed requires a smaller contention window W and maximum backoff stage m to achieve the maximum throughput. Finally, it can be observed that, for the same configuration of (N, M, m), the basic access mechanism slightly outperforms the RTS/CTS access mechanism, whereas the RTS/CTS access mechanism can achieve the optimal normalized throughput at lower W compared with the basic access mechanism.

VII. CONCLUSION

In this paper, we have proposed MAC protocols for CR networks that explicitly take into account spectrum-sensing performance. In particular, we have derived the normalized throughput of the proposed MAC protocols and determined their optimal configuration for throughput maximization. These studies have been performed for both single- and multiple-channel scenarios subject to protection constraints for primary receivers. Finally, we have presented numerical results to confirm important theoretical findings in this paper and to show significant performance gains that were achieved by the optimal configuration for the proposed MAC protocols.

APPENDIX A
PROOF OF PROPOSITION 1

We start the proof by defining the following two quantities: 1) $\varphi^j := -(\alpha^j + \sqrt{\tau f_s}\gamma^j)^2/2$, and 2) $c_{n_0} := \mathcal{P}_s \mathcal{P}_t PS/T$. Taking the derivative of $\mathcal{NT}$ versus τ, we have

$$\frac{\partial \mathcal{NT}}{\partial \tau} = \sum_{n_0=1}^{N} c_{n_0} \sum_{k=1}^{C_N^{n_0}} \times \left\{ \left(\frac{-1}{\bar{T}_{sd}}\right) \prod_{i\in\mathcal{S}_k} \mathcal{P}^i_{idle} \prod_{j\in\mathcal{S}\setminus\mathcal{S}_k} \mathcal{P}^j_{busy} + \left\lfloor \frac{T-\tau}{\bar{T}_{sd}} \right\rfloor \sqrt{\frac{f_s}{8\pi\tau}} \times \left[\sum_{i\in\mathcal{S}_k} \gamma^i \exp(\varphi^i) \mathcal{P}^i(\mathcal{H}_0) \times \prod_{l\in\mathcal{S}_k\setminus i} \mathcal{P}^l_{idle} \prod_{j\in\mathcal{S}\setminus\mathcal{S}_k} \mathcal{P}^j_{busy} - \sum_{j\in\mathcal{S}\setminus\mathcal{S}_k} \gamma^j \exp(\varphi^j) \mathcal{P}^j(\mathcal{H}_0) \times \prod_{l\in\mathcal{S}\setminus\mathcal{S}_k\setminus j} \mathcal{P}^l_{busy} \prod_{i\in\mathcal{S}_k} \mathcal{P}^i_{idle} \right] \right\}. \quad (32)$$

Based on this expression, we have

$$\lim_{\tau\to T} \frac{\partial \mathcal{NT}}{\partial \tau} = \sum_{n_0=1}^{N} c_{n_0} \sum_{k=1}^{C_N^{n_0}} \left(\frac{-1}{\bar{T}_{sd}}\right) \prod_{i\in\mathcal{S}_k} \mathcal{P}^i_{idle} \prod_{j\in\mathcal{S}\setminus\mathcal{S}_k} \mathcal{P}^j_{busy} < 0. \quad (33)$$

Now, let us define the following quantity:

$$\mathcal{K}_\tau \triangleq \sum_{n_0=1}^{N} c_{n_0} \sum_{k=1}^{C_N^{n_0}} \left[\sum_{i\in\mathcal{S}_k} \gamma^i \exp(\varphi^i) \mathcal{P}^i(\mathcal{H}_0) \prod_{l\in\mathcal{S}_k\setminus i} \mathcal{P}^l_{idle} \prod_{j\in\mathcal{S}\setminus\mathcal{S}_k} \mathcal{P}^j_{busy} - \sum_{j\in\mathcal{S}\setminus\mathcal{S}_k} \gamma^j \exp(\varphi^j) \mathcal{P}^j(\mathcal{H}_0) \prod_{l\in\mathcal{S}\setminus\mathcal{S}_k\setminus j} \mathcal{P}^l_{busy} \prod_{i\in\mathcal{S}_k} \mathcal{P}^i_{idle} \right]. \quad (34)$$

Then, it can be shown that $\mathcal{K}_\tau > 0$, as explained in the following discussion. First, it can be verified that the term c_{n_0} is almost a constant for different n_0. Therefore, to highlight the intuition behind the underlying property (i.e., $\mathcal{K}_\tau > 0$), we substitute $\mathcal{K} = c_{n_0}$ into the aforementioned equation. Then, $\mathcal{K}_\tau$ in (34) reduces to

$$\mathcal{K}_\tau = \mathcal{K}_a \sum_{n_0=1}^{N} C_N^{n_0} \left(n_0 \mathcal{P}_{idle}^{n_0-1} \mathcal{P}_{busy}^{N-n_0} - (N-n_0) \mathcal{P}_{busy}^{N-n_0-1} \right) \quad (35)$$

where $\mathcal{K}_a = \mathcal{K}\gamma \exp(\varphi) \mathcal{P}(\mathcal{H}_0)$. Let us define the following quantities: $x = \mathcal{P}_{busy}$, $x \in \mathbb{R}_x \triangleq [\mathcal{P}_d \mathcal{P}(\mathcal{H}_1), \mathcal{P}(\mathcal{H}_0) + \mathcal{P}_d \mathcal{P}(\mathcal{H}_1)]$. After some manipulations, we have

$$\mathcal{K}_\tau = \mathcal{K}_a \sum_{n_0=1}^{N} f(x) \left(\frac{n_0}{x(1-x)} - \frac{N}{x} \right) \quad (36)$$

where $f(x) = C_N^{n_0} (1-x)^{n_0} x^{N-n_0}$ is the binomial mass function [28], with $p = 1-x$ and $q = x$. Because the total probabilities and the mean of this binomial distribution are 1 and $Np = N(1-x)$, respectively, we have

$$\sum_{n_0=0}^{N} f(x) = 1 \quad (37)$$

$$\sum_{n_0=0}^{N} n_0 f(x) = N(1-x). \quad (38)$$

It can be observed that, in (36), the element that corresponds to $n_0 = 0$ is missing. Applying the results in (37) and (38) to (36), we have

$$\mathcal{K}_\tau = \mathcal{K}_a N x^{N-1} > 0 \quad \forall x. \quad (39)$$

Therefore, we have

$$\lim_{\tau \to 0} \frac{\partial \mathcal{NT}}{\partial \tau} = +\infty. \quad (40)$$

Hence, we have completed the proof for the first two properties of Proposition 1.

To prove the third property, let us find the solution of $\partial \mathcal{NT} / \partial \tau = 0$. After some simple manipulations and using the properties of the binomial distribution, this equation reduces to

$$h(\tau) = g(\tau) \quad (41)$$

where

$$g(\tau) = (\alpha + \gamma \sqrt{f_s \tau})^2 \quad (42)$$

$$h(\tau) = 2 \log \left(\mathcal{P}(\mathcal{H}_0) \gamma \sqrt{\frac{f_s}{8\pi}} \frac{T-\tau}{\sqrt{\tau}} \right) + h_1(x) \quad (43)$$

where $h_1(x) = 2 \log((\mathcal{K}_\tau / \mathcal{K}_a) / \sum_{n_0=1}^{N} C_N^{n_0} f(x)) = 2 \log(N x^{N-1} / 1 - x^N)$.

To prove the third property, we will show that $h(\tau)$ intersects $g(\tau)$ only once. We first state one important property of $h(\tau)$ in the following lemma.

Lemma 1: $h(\tau)$ is a decreasing function.

Proof: Taking the first derivative of $h(.)$, we have

$$\frac{\partial h}{\partial \tau} = \frac{-1}{\tau} - \frac{2}{T-\tau} + \frac{\partial h_1}{\partial x} \frac{\partial x}{\partial \tau}. \quad (44)$$

We now derive $\partial x / \partial \tau$ and $\partial h_1 / \partial x$ as follows:

$$\frac{\partial x}{\partial \tau} = -\mathcal{P}(\mathcal{H}_0) \gamma \sqrt{\frac{f_s}{8\pi\tau}} \exp\left(-\frac{(\alpha + \gamma\sqrt{f_s \tau})^2}{2} \right) < 0 \quad (45)$$

$$\frac{\partial h_1}{\partial x} = 2 \frac{N-1+x^N}{x(1-x^N)} > 0. \quad (46)$$

Hence, $(\partial h_1 / \partial x)(\partial x / \partial \tau) < 0$. Using this result in (44), we have $(\partial h / \partial \tau) < 0$. Therefore, we can conclude that $h(\tau)$ is monotonically decreasing. ■

We now consider function $g(\tau)$. Taking the derivative of $g(\tau)$, we have

$$\frac{\partial g}{\partial \tau} = (\alpha + \gamma \sqrt{f_s \tau}) \frac{\gamma \sqrt{f_s}}{\sqrt{\tau}}. \quad (47)$$

Therefore, the monotonicity property of $g(\tau)$ depends only on $y = \alpha + \gamma \sqrt{f_s \tau}$. Properties 1 and 2 imply that there must be at least one intersection between $h(\tau)$ and $g(\tau)$. We now prove that there is, indeed, a unique intersection. To proceed, we consider two different regions for τ as follows:

$$\mathbf{\Omega}_1 = \{\tau | \alpha + \gamma \sqrt{f_s \tau} < 0, \tau \leq T\} = \left\{ 0 < \tau < \frac{\alpha^2}{\gamma^2 f_s} \right\}$$

$$\mathbf{\Omega}_2 = \{\tau | \alpha + \gamma \sqrt{f_s \tau} \geq 0, \tau \leq T\} = \left\{ \frac{\alpha^2}{\gamma^2 f_s} \leq \tau \leq T \right\}.$$

Based on the definitions of these two regions, we have that $g(\tau)$ decreases in $\mathbf{\Omega}_1$ and increases in $\mathbf{\Omega}_2$. To show that there is a unique intersection between $h(\tau)$ and $g(\tau)$, we prove the following lemma.

Lemma 2: The following statements are correct.

1) If there is an intersection between $h(\tau)$ and $g(\tau)$ in $\mathbf{\Omega}_2$, then it is the only intersection in this region, and there is no intersection in $\mathbf{\Omega}_1$.
2) If there is an intersection between $h(\tau)$ and $g(\tau)$ in $\mathbf{\Omega}_1$, then it is the only intersection in this region, and there is no intersection in $\mathbf{\Omega}_2$.

Proof: We now prove the first statement. Recall that $g(\tau)$ monotonically increases in $\mathbf{\Omega}_2$; therefore, $g(\tau)$ and $h(\tau)$ can intersect at most once in this region (because $h(\tau)$ decreases). In addition, $g(\tau)$ and $h(\tau)$ cannot intersect in $\mathbf{\Omega}_1$ for this case if we can prove that $\partial h / \partial \tau < \partial g / \partial \tau$. This is because both functions decrease in $\mathbf{\Omega}_1$. We will prove that $\partial h / \partial \tau < \partial g / \partial \tau$ in Lemma 3 after this proof.

We now prove the second statement of Lemma 2. Recall that we have $\partial h / \partial \tau < \partial g / \partial \tau$. Therefore, there is at most one intersection between $g(\tau)$ and $h(\tau)$ in $\mathbf{\Omega}_1$. In addition, it is clear that there cannot be any intersection between these two functions in $\mathbf{\Omega}_2$ for this case. ■

Lemma 3: We have $\partial h / \partial \tau < \partial g / \partial \tau$.

Proof: Based on (44), we can see that Lemma 3 holds if we can prove the following stronger result:

$$\frac{-1}{\tau} + \frac{\partial h_1}{\partial \tau} < \frac{\partial g}{\partial \tau} \quad (48)$$

where $\partial h_1 / \partial \tau = (\partial h_1 / \partial x)(\partial x / \partial \tau)$, $\partial x / \partial \tau$ is derived in (45), $\partial h_1 / \partial x$ is derived in (46), and $\partial g / \partial \tau$ is given in (47).

To prove (48), we will prove the following expression:

$$-\frac{1}{\tau}+\frac{y\mathcal{P}(\mathcal{H}_0)\gamma\sqrt{\frac{f_s}{\tau}}}{\mathcal{P}(\mathcal{H}_0)+\sqrt{2\pi}\mathcal{P}(\mathcal{H}_1)(1-\bar{\mathcal{P}}_d)(-y)\exp\left(\frac{y^2}{2}\right)}<\frac{\partial g}{\partial \tau} \quad (49)$$

where $y=(\alpha+\gamma\sqrt{f_s\tau}<0)$. Then, we show that

$$\frac{\partial h_1}{\partial \tau}<\frac{y\mathcal{P}(\mathcal{H}_0)\gamma\sqrt{\frac{f_s}{\tau}}}{\mathcal{P}(\mathcal{H}_0)+\sqrt{2\pi}\mathcal{P}(\mathcal{H}_1)(1-\bar{\mathcal{P}}_d)(-y)\exp\left(\frac{y^2}{2}\right)}. \quad (50)$$

Therefore, the result in (48) will hold. Let us first prove (50). First, let us prove the following expression:

$$\frac{\partial h_1}{\partial x}>\frac{2}{1-x}. \quad (51)$$

Using the result in $\partial h_1/\partial x$ based on (46), (51) is equivalent to

$$2\frac{N-1+x^N}{x(1-x^N)}>\frac{2}{1-x}. \quad (52)$$

After some manipulations, we get

$$(1-x)\left(N-1-(x+x^2+\cdots+x^{N-1})\right)>0. \quad (53)$$

It can be observed that $0<x<1$ and $0<x^i<1$, $i\in[1,N-1]$. Thus, $N-1-(x+x^2+\cdots+x^{(N-1)})>0$; hence, (53) holds. Therefore, we have completed the proof for (51).

We now show that the following inequality holds:

$$\frac{2}{1-x}>\frac{2\sqrt{2\pi}(-y)\exp\left(\frac{y^2}{2}\right)}{\mathcal{P}(\mathcal{H}_0)+\sqrt{2\pi}\mathcal{P}(\mathcal{H}_1)(1-\bar{\mathcal{P}}_d)(-y)\exp\left(\frac{y^2}{2}\right)}. \quad (54)$$

This inequality can be proved as follows. In [26], it has been shown that $\mathcal{Q}(t)$ with $t>0$ satisfies

$$\frac{1}{\mathcal{Q}(t)}>\sqrt{2\pi}t\exp\left(\frac{t^2}{2}\right). \quad (55)$$

Applying this result to $\mathcal{P}_f=\mathcal{Q}(y)=1-\mathcal{Q}(-y)$, with $y=(\alpha+\gamma\sqrt{f_s\tau})<0$, we have

$$\frac{1}{1-P_f}>\sqrt{2\pi}(-y)\exp\left(\frac{y^2}{2}\right). \quad (56)$$

After some manipulations, we obtain

$$\mathcal{P}_f>1-\frac{1}{\sqrt{2\pi}(-y)\exp\left(\frac{y^2}{2}\right)}. \quad (57)$$

Recall that we have defined $x=\mathcal{P}_f\mathcal{P}(\mathcal{H}_0)+\bar{\mathcal{P}}_d\mathcal{P}(\mathcal{H}_1)$. Using the result in (57), we can obtain the lower bound of $2/(1-x)$, as given in (54). Using the results in (51) and (54) and the fact that $(\partial x/\partial\tau)<0$, we finally complete the proof for (50).

To complete the proof of the lemma, we need to prove that (49) holds. Substituting $\partial g/\partial\tau$ based on (47) to (49) and making some further manipulations, we have

$$\frac{-1}{y(y-\alpha)}>1-\frac{y\mathcal{P}(\mathcal{H}_0)\gamma\sqrt{\frac{f_s}{\tau}}}{\mathcal{P}(\mathcal{H}_0)+\sqrt{2\pi}\mathcal{P}(\mathcal{H}_1)(1-\bar{\mathcal{P}}_d)(-y)\exp\left(\frac{y^2}{2}\right)}. \quad (58)$$

Let us consider the left-hand side (LHS) of (58). We have $0<y-\alpha=\gamma\sqrt{f_s\tau}<-\alpha$; therefore, we have $0<-y<-\alpha$. Applying the Cauchy–Schwarz inequality to $-y$ and $y-\alpha$, we have

$$0<-y(y-\alpha)\le\left(\frac{-y+y-\alpha}{2}\right)^2=\frac{\alpha^2}{4}. \quad (59)$$

Hence

$$\frac{1}{-y(y-\alpha)}\ge\frac{4}{\alpha^2}=\frac{4}{(2\gamma+1)\left(\mathcal{Q}^{-1}(\bar{\mathcal{P}}_d)\right)^2}>1. \quad (60)$$

It can be observed that the right-hand side (RHS) of (58) is less than 1. Therefore, (58) holds, which implies that (48) and (49) also hold. ■

Finally, the last property holds, because $\Pr(n=n_0)<1$ and the conditional throughput are all bounded from above. Therefore, we have completed the proof of Proposition 1.

Appendix B
Proof of Proposition 2

To prove the properties stated in Proposition 2, we first find the derivative of $\widetilde{\mathcal{NT}}(\tau)$. Again, it can be verified that $\mathcal{P}_t\mathcal{P}_sPS/T$ is almost a constant for different n_0. To demonstrate the proof for the proposition, we substitute this term as a constant value, denoted as $\mathcal{K}$, in the throughput formula. In addition, for large T, $\lfloor T-\tau/\bar{T}_{sd}\rfloor$ is very close to $T-\tau/\bar{T}_{sd}$. Therefore, $\widetilde{\mathcal{NT}}$ can accurately be approximated as

$$\widetilde{\mathcal{NT}}(\tau)=\sum_{n_0=1}^{N}\mathcal{K}C_N^{n_0}(T-\tau)(1-x^M)^{n_0}x^{M(N-n_0)}(1-x) \quad (61)$$

where $\mathcal{K}=P_tP_sPS/T$, and $x=P_{busy}$. Now, let us define the following function:

$$f'(x)=(1-x^M)^{n_0}x^{M(N-n_0)}(1-x). \quad (62)$$

Then, we have

$$\frac{\partial f'}{\partial x}=f'(x)\left[\frac{-1}{1-x}-\frac{Mn_0}{1-x^M}x^{M-1}+\frac{M(N-n_0)}{x}\right]. \quad (63)$$

In addition, $\partial x/\partial\tau$ is the same as (45). Hence, the first derivation of $\widetilde{\mathcal{NT}}(\tau)$ can be written as

$$\begin{aligned}\frac{\partial\widetilde{\mathcal{NT}}(\tau)}{\partial\tau}&=\sum_{n_0=1}^{N}\mathcal{K}C_N^{n_0}\left[-f'(x)+(T-\tau)\frac{\partial f'}{\partial x}\frac{\partial x}{\partial\tau}\right]\\&=\sum_{n_0=1}^{N}\mathcal{K}C_N^{n_0}f'(x)\\&\quad\times\Bigg[(T-\tau)\left[\frac{1}{1-x}+\frac{Mn_0}{1-x^M}x^{M-1}-\frac{M(N-n_0)}{x}\right]\\&\quad\times\mathcal{P}(\mathcal{H}_0)\gamma\sqrt{\frac{f_s}{8\pi\tau}}\exp\left(-\frac{(\alpha+\gamma\sqrt{f_s\tau})^2}{2}\right)-1\Bigg].\end{aligned} \quad (64)$$

Based on (23), the range of x, i.e., $\mathbb{R}_x$, can be expressed as $[\mathcal{P}_d\mathcal{P}(\mathcal{H}_1), \mathcal{P}(\mathcal{H}_0) + \mathcal{P}_d\mathcal{P}(\mathcal{H}_1)]$. Now, it can be observed that

$$\lim_{\tau\to T} \frac{\partial \widetilde{\mathcal{NT}}(\tau)}{\partial \tau} = -\sum_{n_0=1}^{N} \mathcal{K} C_N^{n_0} f'(x) < 0. \tag{65}$$

Therefore, the second property of Proposition 2 holds.

Now, let us define the following quantity:

$$\mathcal{K}'_\tau = \sum_{n_0=1}^{N} C_N^{n_0} f'(x) \left[\frac{1}{1-x} + \frac{M n_0 x^{M-1}}{1-x^M} - \frac{M(N-n_0)}{x}\right]. \tag{66}$$

Then, it is shown that $\lim_{\tau\to 0}(\partial\widetilde{\mathcal{NT}}(\tau)/\partial\tau) = +\infty > 0$ if $\mathcal{K}'_\tau > 0 \forall M$, N, and $x \in \mathbb{R}_x$. This last property is stated and proved in the following lemma.

Lemma 4: $\mathcal{K}'_\tau > 0, \forall M, N$, and $x \in \mathbb{R}_x$.

Proof: Making some manipulations to (66), we have

$$\mathcal{K}'_\tau = \left(1 - \frac{(1-x)M}{x}\right) \sum_{n_0=1}^{N} C_N^{n_0} (1-x^M)^{n_0} x^{M(N-n_0)} + \frac{M(1-x)}{x(1-x^M)} \sum_{n_0=1}^{N} C_N^{n_0} n_0 (1-x^M)^{n_0} x^{M(N-n_0)}. \tag{67}$$

It can be observed that $\sum_{n_0=1}^{N} C_N^{n_0}(1-x^M)^{n_0}x^{M(N-n_0)}$ and $\sum_{n_0=1}^{N} C_N^{n_0} n_0(1-x^M)^{n_0}x^{M(N-n_0)}$ represent a cumulative distribution function (cdf) and the mean of a binomial distribution [28], respectively, with parameter p missing the term that corresponds to $n_0 = 0$, where $p = 1 - x^M$. Note that the cdf and mean of such a distribution are 1 and $Np = N(1 - x^M)$, respectively. Hence, (67) can be rewritten as

$$\mathcal{K}'_\tau = \left(1 - \frac{(1-x)M}{x}\right)(1-x^{MN}) + \frac{M(1-x)}{x(1-x^M)} N(1-x^M). \tag{68}$$

After some manipulations, we have

$$\mathcal{K}'_\tau = 1 - x^{MN} + MNx^{MN-1}(1-x) > 0 \quad \forall x. \tag{69}$$

Therefore, we have completed the proof. ■

Hence, the first property of Proposition 1 also holds.

To prove the third property, let us consider the following equation: $\partial\widetilde{\mathcal{NT}}(\tau)/\partial\tau = 0$. After some manipulations, we have the following equivalent equation:

$$g(\tau) = h'(\tau) \tag{70}$$

where

$$g(\tau) = (\alpha + \gamma\sqrt{f_s\tau})^2 \tag{71}$$

$$h'(\tau) = 2\log\left(\mathcal{P}(\mathcal{H}_0)\gamma\sqrt{\frac{f_s}{8\pi}}\frac{T-\tau}{\sqrt{\tau}}\right) + h'_1(x) \tag{72}$$

$$h'_1(x) = 2\log\frac{\mathcal{K}'_\tau}{\sum\limits_{n_0=1}^{N} C_N^{n_0} f'(x)}. \tag{73}$$

K'_τ is given in (66). We have the following result for $h'(\tau)$.

Lemma 5: $h'(\tau)$ monotonically decreases in τ.

Proof: The derivative of $h'(\tau)$ can be written as

$$\frac{\partial h'}{\partial \tau} = \frac{-1}{\tau} - \frac{2}{T-\tau} + \frac{\partial h'_1}{\partial \tau}. \tag{74}$$

In the following discussion, we will show that $(\partial h'_1/\partial x) > 0$ for all $x \in \mathbb{R}_x$, all M and N, and $(\partial x/\partial\tau) < 0$. Hence, $\partial h'_1/\partial\tau = (\partial h'_1/\partial x)(\partial x/\partial \tau) < 0$. Based on this condition, we have $\partial h'/\partial\tau < 0$; therefore, the property stated in Lemma 5 holds.

We now show that $\partial h'_1/\partial x > 0$ for all $x \in \mathbb{R}_x$, all M, and N. Substituting $\mathcal{K}'_\tau$ in (69) to (73) and exploiting the property of the cdf of the binomial distribution function, we have

$$\begin{aligned} h'_1(x) &= 2\log\frac{1 - x^{MN} + MNx^{MN-1}(1-x)}{(1-x)\sum_{n_0=1}^{N} C_N^{n_0}(1-x^M)^{n_0}x^{M(N-n_0)}} \\ &= 2\log\frac{1 - x^{MN} + MNx^{MN-1}(1-x)}{(1-x)(1-x^{MN})}. \end{aligned} \tag{75}$$

Taking the first derivative of $h'_1(x)$ and performing some manipulations, we obtain

$$\frac{\partial h'_1}{\partial x} = 2\frac{\left(r(r-1)x^{r-2}(1-x)^2(1-x^r) + (1-x^r)^2 + r^2x^{2(r-1)}(1-x)^2\right)}{\left(1-x^r+rx^{(r-1)}(1-x)\right)(1-x)(1-x^r)} \tag{76}$$

where $r = MN$. It can be observed that there is no negative term in (76); hence, $(\partial h'_1/\partial x) > 0$ for all $x \in \mathbb{R}_x$, all M, and N. Therefore, we have proved the lemma. ■

To prove the third property, we show that $g(\tau)$ and $h'(\tau)$ intersect only once in the range of $[0, T]$. This approach will be done using the same approach as in Appendix A. In particular, we will consider the two regions $\mathbf{\Omega}_1$ and $\mathbf{\Omega}_2$ and prove two properties stated in Lemma 2 for this case. As shown in Appendix A, the third property holds if we can prove that $-(1/\tau) + (\partial h'_1/\partial\tau) < (\partial g/\partial\tau)$. It can be observed that all steps that were used to prove this inequality are the same as the steps in the proof of (48) for Proposition 1. Hence, we need to prove

$$\frac{\partial h'_1}{\partial x} > \frac{2}{1-x}. \tag{77}$$

Substituting $\partial h'_1/\partial x$ based on (76) to (77), this inequality reduces to

$$2\frac{\left(r(r-1)x^{r-2}(1-x)^2(1-x^r) + (1-x^r)^2 + r^2x^{2(r-1)}(1-x)^2\right)}{\left(1-x^r+rx^{(r-1)}(1-x)\right)(1-x)(1-x^r)} > \frac{2}{1-x}. \tag{78}$$

After some manipulations, this inequality becomes equivalent to

$$rx^{(r-2)}(1-x)^2\left[r - \left(1+x+x^2+\cdots+x^{(r-1)}\right)\right] > 0. \tag{79}$$

It can be observed that $0 < x < 1$ and $0 < x^i < 1$, $i \in [0, r-1]$. Hence, we have $r - (1 + x + x^2 + \cdots + x^{(r-1)}) > 0$, which shows that (79), indeed, holds. Therefore, (77) holds, and we have completed the proof of the third property. Finally, the last property of the Proposition is obviously correct. Hence, we have completed the proof of Proposition 2.

References

[1] Q. Zhao and B. M. Sadler, "A survey of dynamic spectrum access," *IEEE Signal Process. Mag.*, vol. 24, no. 3, pp. 79–89, May 2007.

[2] C. Stevenson, G. Chouinard, Z. Lei, W. Hu, S. Shellhammer, and W. Caldwell, "IEEE 802.22: The first cognitive radio wireless regional area network standard," *IEEE Commun. Mag.*, vol. 47, no. 1, pp. 130–138, Jan. 2009.

[3] D. I. Kim, L. B. Le, and E. Hossain, "Joint rate and power allocation for cognitive radios in dynamic spectrum access environment," *IEEE Trans. Wireless Commun.*, vol. 7, no. 12, pp. 5517–5527, Dec. 2008.

[4] L. B. Le and E. Hossain, "Resource allocation for spectrum underlay in cognitive radio networks," *IEEE Trans. Wireless Commun.*, vol. 7, no. 12, pp. 5306–5315, Dec. 2008.

[5] Y.-C. Liang, Y. Zeng, E. C. Y. Peh, and A. T. Hoang, "Sensing-throughput tradeoff for cognitive radio networks," *IEEE Trans. Wireless Commun.*, vol. 7, no. 4, pp. 1326–1337, Apr. 2008.

[6] E. C. Y. Peh, Y.-C. Liang, and Y. L. Guan, "Optimization of cooperative sensing in cognitive radio networks: A sensing-throughput tradeoff view," in *Proc. IEEE Int. Conf. Commun.*, 2009, pp. 3521–3525.

[7] N. Devroye, P. Mitran, and V. Tarokh, "Achievable rates in cognitive radio channels," *IEEE Trans. Inf. Theory*, vol. 52, no. 5, pp. 1813–1827, May 2006.

[8] F. Wang, M. Krunz, and S. Cui, "Price-based spectrum management in cognitive radio networks," *IEEE J. Sel. Topics Signal Process.*, vol. 2, no. 1, pp. 74–87, Feb. 2008.

[9] D. Niyato and E. Hossain, "Competitive pricing for spectrum sharing in cognitive radio networks: Dynamic game, inefficiency of Nash equilibrium, and collusion," *IEEE J. Sel. Areas Commun.*, vol. 26, no. 1, pp. 192–202, Jan. 2008.

[10] T. Yucek and H. Arslan, "A survey of spectrum sensing algorithms for cognitive radio applications," *IEEE Commun. Surveys Tuts.*, vol. 11, no. 1, pp. 116–130, First Quarter, 2009.

[11] J. Unnikrishnan and V. V. Veeravalli, "Cooperative sensing for primary detection in cognitive radio," *IEEE J. Sel. Topics Signal Process.*, vol. 2, no. 1, pp. 18–27, Feb. 2008.

[12] C. Cormio and K. R. Chowdhury, "A survey on MAC protocols for cognitive radio networks," *Ad Hoc Netw.*, vol. 7, no. 7, pp. 1315–1329, Sep. 2009.

[13] H. Kim and K. G. Shin, "Efficient discovery of spectrum opportunities with MAC-layer sensing in cognitive radio networks," *IEEE Trans. Mobile Comput.*, vol. 7, no. 5, pp. 533–545, May 2008.

[14] H. Su and X. Zhang, "Opportunistic MAC protocols for cognitive radio based wireless networks," in *Proc. CISS*, 2007, pp. 363–368.

[15] H. Nan, T.-I. Hyon, and S.-J. Yoo, "Distributed coordinated spectrum sharing MAC protocol for cognitive radio," in *Proc. IEEE DySPAN*, 2007, pp. 240–249.

[16] C. Cordeiro and K. Challapali, "C-MAC: A cognitive MAC protocol for multichannel wireless networks," in *Proc. IEEE DySPAN*, 2007, pp. 147–157.

[17] Y. R. Kondareddy and P. Agrawal, "Synchronized MAC protocol for multi-hop cognitive radio networks," in *Proc. IEEE ICC*, 2008, pp. 3198–3202.

[18] A. C.-C. Hsu, D. S. L. Weit, and C.-C. J. Kuo, "A cognitive MAC protocol using statistical channel allocation for wireless ad hoc networks," in *Proc. IEEE WCNC*, 2007, pp. 105–110.

[19] H. Su and X. Zhang, "Cross-layer-based opportunistic MAC protocols for QoS provisionings over cognitive radio wireless networks," *IEEE J. Sel. Areas Commun.*, vol. 26, no. 1, pp. 118–129, Jan. 2008.

[20] Y. Zuo, Y.-D. Yao, and B. Zheng, "Outage probability analysis of cognitive transmissions: Impact of spectrum sensing overhead," *IEEE Trans. Wireless Commun.*, vol. 9, no. 8, pp. 2676–2688, Aug. 2010.

[21] Y. Zou, Y.-D. Yao, and B. Zheng, "Cognitive transmissions with multiple relays in cognitive radio networks," *IEEE Trans. Wireless Commun.*, vol. 10, no. 2, pp. 648–659, Feb. 2011.

[22] Y. Zou, Y.-D. Yao, and B. Zheng, "A selective-relay-based cooperative spectrum sensing scheme without dedicated reporting channels in cognitive radio networks," *IEEE Trans. Wireless Commun.*, vol. 10, no. 4, pp. 1188–1198, Apr. 2011.

[23] J. Shi, E. Aryafar, T. Salonidis, and E. W. Knightly, "Synchronized CSMA contention: Model, implementation and evaluation," in *Proc. IEEE INFOCOM*, 2009, pp. 2052–2060.

[24] G. Bianchi, "Performance analysis of the IEEE 802.11 distributed coordination function," *IEEE J. Sel. Areas Commun.*, vol. 18, no. 3, pp. 535–547, Mar. 2000.

[25] S. Kameshwaran and Y. Narahari, "Nonconvex piecewise linear knapsack problems," *Eur. J. Oper. Res.*, vol. 192, no. 1, pp. 56–68, Jan. 2009.

[26] G. K. Karagiannidis and A. S. Lioumpas, "An improved approximation for the Gaussian Q-function," *IEEE Commun. Lett.*, vol. 11, no. 8, pp. 644–646, Aug. 2007.

[27] S. P. Boyd and L. Vandenberghe, *Convex Optimization*. Cambridge, U.K.: Cambridge Univ. Press, 2004.

[28] V. Krishnan, *Probability and Random Processes*. Hoboken, NJ: Wiley-Interscience, 2006, p. xiii.

Le Thanh Tan (S'11) received the B.Eng. and M.Eng. degrees from Ho Chi Minh City University of Technology, Ho Chi Minh City, Vietnam, in 2002 and 2004, respectively. He is currently working toward the Ph.D. degree with the Institut National de la Recherche Scientifique—Énergie, Matériaux et Télécommunications, Université du Québec, Montréal, QC, Canada.

From 2002 to 2010, he was a Lecturer with the University of Technical Education, Ho Chi Minh City. His research interests include wireless communications and networking, cognitive radios (protocol design, spectrum sensing, detection, and estimation), statistical signal processing, random matrix theory, compressed sensing, and compressed sampling.

Long Bao Le (S'04–M'07) received the B.Eng. (with the highest distinction) degree from Ho Chi Minh City University of Technology, Ho Chi Minh City, Vietnam, in 1999, the M.Eng. degree from the Asian Institute of Technology, Pathumthani, Thailand, in 2002, and the Ph.D. degree from the University of Manitoba, Winnipeg, MB, Canada, in 2007.

He was a Postdoctoral Researcher, first with the University of Waterloo, Waterloo, ON, Canada, and then with Massachusetts Institute of Technology, Cambridge. He is currently an Assistant Professor with the Institut National de la Recherche Scientifique—Énergie, Matériaux et Télécommunications, Université du Québec, Montréal, QC, Canada. His research interests include cognitive radio, dynamic spectrum sharing, cooperative diversity and relay networks, stochastic control, and cross-layer design for communication networks.